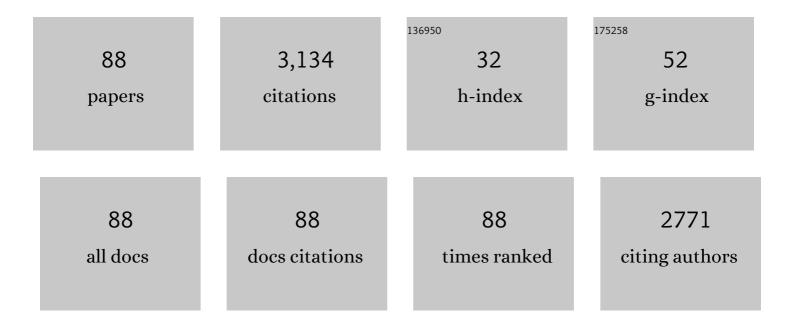
Hao Qiu

List of Publications by Year in descending order

Source: https://exaly.com/author-pdf/4666745/publications.pdf Version: 2024-02-01



Ηλο Οιμ

#	Article	IF	CITATIONS
1	Dispersion and transport of microplastics in three water-saturated coastal soils. Journal of Hazardous Materials, 2022, 424, 127614.	12.4	12
2	Incorporation of chemical and toxicological availability into metal mixture toxicity modeling: State of the art and future perspectives. Critical Reviews in Environmental Science and Technology, 2022, 52, 1730-1772.	12.8	8
3	Modeling and visualizing the transport and retention of cationic and oxyanionic metals (Cd and Cr) in saturated soil under various hydrochemical and hydrodynamic conditions. Science of the Total Environment, 2022, 812, 151467.	8.0	14
4	Lanthanum and cerium disrupt similar biological pathways and interact synergistically in Triticum aestivum as revealed by metabolomic profiling and quantitative modeling. Journal of Hazardous Materials, 2022, 426, 127831.	12.4	10
5	Contrasting effects of dry-wet and freeze-thaw aging on the immobilization of As in As-contaminated soils amended by zero-valent iron-embedded biochar. Journal of Hazardous Materials, 2022, 426, 128123.	12.4	20
6	Evaluation of long-term carbon sequestration of biochar in soil with biogeochemical field model. Science of the Total Environment, 2022, 822, 153576.	8.0	24
7	Rapid reactivation of aged NZVI/GO by Shewanella CN32 for efficient removal of tetrabromobisphenol A and associated reaction mechanisms. Journal of Cleaner Production, 2022, 333, 130215.	9.3	6
8	Direct and Indirect Electron Transfer Routes of Chromium(VI) Reduction with Different Crystalline Ferric Oxyhydroxides in the Presence of Pyrogenic Carbon. Environmental Science & Technology, 2022, 56, 1724-1735.	10.0	40
9	Editorial for Special Issue "Elemental Concentration and Pollution in Soil, Water, and Sedimentâ€. Minerals (Basel, Switzerland), 2022, 12, 338.	2.0	0
10	Development of phosphorus composite biochar for simultaneous enhanced carbon sink and heavy metal immobilization in soil. Science of the Total Environment, 2022, 831, 154845.	8.0	28
11	Plant intelligence in a rapidly changing world: Implementation of plant-plant communications in managed plant systems. , 2022, 2, 100008.		2
12	UV/ozone induced physicochemical transformations of polystyrene nanoparticles and their aggregation tendency and kinetics with natural organic matter in aqueous systems. Journal of Hazardous Materials, 2022, 433, 128790.	12.4	18
13	Commonwealth of Soil Health: How Do Earthworms Modify the Soil Microbial Responses to CeO ₂ Nanoparticles?. Environmental Science & Technology, 2022, 56, 1138-1148.	10.0	17
14	Metal resistant gut microbiota facilitates snails feeding on metal hyperaccumulator plant Sedum alfredii in the phytoremediation field. Ecotoxicology and Environmental Safety, 2022, 236, 113514.	6.0	7
15	Colloid formation and facilitated chromium transport in the coastal area soil induced by freshwater and seawater alternating fluctuations. Water Research, 2022, 218, 118456.	11.3	10
16	Smart 6S roadmap for deciphering the migration and risk of heavy metals in soil and groundwater systems at brownfield sites nationwide in China. Science Bulletin, 2022, 67, 1295-1299.	9.0	10
17	Oil spills enhanced dispersion and transport of microplastics in sea water and sand at coastal beachheads. Journal of Hazardous Materials, 2022, 436, 129312.	12.4	4
18	Multiomics analyses uncover nanoceria triggered oxidative injury and nutrient imbalance in earthworm Eisenia fetida. Journal of Hazardous Materials, 2022, 437, 129354.	12.4	11

ΗΑΟ QIU

#	Article	IF	CITATIONS
19	Dynamic release and transformation of metallic copper colloids in flooded paddy soil: Role of soil reducible sulfate and temperature. Journal of Hazardous Materials, 2021, 402, 123462.	12.4	8
20	The crucial role of a protein corona in determining the aggregation kinetics and colloidal stability of polystyrene nanoplastics. Water Research, 2021, 190, 116742.	11.3	69
21	Application of low dosage of copper oxide and zinc oxide nanoparticles boosts bacterial and fungal communities in soil. Science of the Total Environment, 2021, 757, 143807.	8.0	26
22	Sorption of reactive red by biochars ball milled in different atmospheres: Co-effect of surface morphology and functional groups. Chemical Engineering Journal, 2021, 413, 127468.	12.7	23
23	Nickel-catalyzed formation of mesoporous carbon structure promoted capacitive performance of exhausted biochar. Chemical Engineering Journal, 2021, 406, 126856.	12.7	20
24	Protein corona-induced aggregation of differently sized nanoplastics: impacts of protein type and concentration. Environmental Science: Nano, 2021, 8, 1560-1570.	4.3	28
25	Stabilization of dissolvable biochar by soil minerals: Release reduction and organo-mineral complexes formation. Journal of Hazardous Materials, 2021, 412, 125213.	12.4	41
26	New insights into the underlying influence of bentonite on Pb immobilization by undissolvable and dissolvable fractions of biochar. Science of the Total Environment, 2021, 775, 145824.	8.0	10
27	Persulfate Oxidation of Sulfamethoxazole by Magnetic Iron-Char Composites via Nonradical Pathways: Fe(IV) Versus Surface-Mediated Electron Transfer. Environmental Science & Technology, 2021, 55, 10077-10086.	10.0	180
28	Migration and transformation of chromium in unsaturated soil during groundwater table fluctuations induced by rainfall. Journal of Hazardous Materials, 2021, 416, 126229.	12.4	10
29	Do essential elements (P and Fe) have mitigation roles in the toxicity of individual and binary mixture of yttrium and cerium to Triticum aestivum?. Journal of Hazardous Materials, 2021, 416, 125761.	12.4	8
30	Synergistic role of bulk carbon and iron minerals inherent in the sludge-derived biochar for As(V) immobilization. Chemical Engineering Journal, 2021, 417, 129183.	12.7	18
31	Contribution of pristine and reduced microbial extracellular polymeric substances of different sources to Cu(II) reduction. Journal of Hazardous Materials, 2021, 415, 125616.	12.4	33
32	Dynamic interaction processes of rare earth metal mixtures in terrestrial organisms interpreted by toxicokinetic and toxicodynamic model. Journal of Hazardous Materials, 2021, 418, 126281.	12.4	11
33	Chemical and photo-initiated aging enhances transport risk of microplastics in saturated soils: Key factors, mechanisms, and modeling. Water Research, 2021, 202, 117407.	11.3	59
34	Cytotoxicity and genotoxicity of lanthanides for Vicia faba L. are mediated by their chemical speciation in different exposure media. Science of the Total Environment, 2021, 790, 148223.	8.0	9
35	Microplastics in the soil-groundwater environment: Aging, migration, and co-transport of contaminants $\hat{a} \in $ A critical review. Journal of Hazardous Materials, 2021, 419, 126455.	12.4	212
36	Biomass-derived pyrolytic carbons accelerated Fe(III)/Fe(II) redox cycle for persulfate activation: Pyrolysis temperature-depended performance and mechanisms. Applied Catalysis B: Environmental, 2021, 297, 120446.	20.2	48

ΗΑΟ QIU

#	Article	IF	CITATIONS
37	Mesoporous ball-milling iron-loaded biochar for enhanced sorption of reactive red: Performance and mechanisms. Environmental Pollution, 2021, 290, 117992.	7.5	21
38	Suppressed formation of polycyclic aromatic hydrocarbons (PAHs) during pyrolytic production of Fe-enriched composite biochar. Journal of Hazardous Materials, 2020, 382, 121033.	12.4	43
39	Participation of soil active components in the reduction of Cr(VI) by biochar: Differing effects of iron mineral alone and its combination with organic acid. Journal of Hazardous Materials, 2020, 384, 121455.	12.4	43
40	Model-based rationalization of mixture toxicity and accumulation in Triticum aestivum upon concurrent exposure to yttrium, lanthanum, and cerium. Journal of Hazardous Materials, 2020, 389, 121940.	12.4	6
41	Interactions of CeO2 nanoparticles with natural colloids and electrolytes impact their aggregation kinetics and colloidal stability. Journal of Hazardous Materials, 2020, 386, 121973.	12.4	33
42	The promoted dissolution of copper oxide nanoparticles by dissolved humic acid: Copper complexation over particle dispersion. Chemosphere, 2020, 245, 125612.	8.2	20
43	Bioavailability and phytotoxicity of rare earth metals to Triticum aestivum under various exposure scenarios. Ecotoxicology and Environmental Safety, 2020, 205, 111346.	6.0	6
44	Impact of CeO2 nanoparticles on the aggregation kinetics and stability of polystyrene nanoplastics: Importance of surface functionalization and solution chemistry. Water Research, 2020, 186, 116324.	11.3	59
45	Interactions of arsenic, copper, and zinc in soil-plant system: Partition, uptake and phytotoxicity. Science of the Total Environment, 2020, 745, 140926.	8.0	27
46	Nitrogen Transformation during Pyrolysis of Various N-Containing Biowastes with Participation of Mineral Calcium. ACS Sustainable Chemistry and Engineering, 2020, 8, 12197-12207.	6.7	48
47	One-pot synthesis of nZVI-embedded biochar for remediation of two mining arsenic-contaminated soils: Arsenic immobilization associated with iron transformation. Journal of Hazardous Materials, 2020, 398, 122901.	12.4	109
48	Coupling mixture reference models with DGT-perceived metal flux for deciphering the nonadditive effects of rare earth mixtures to wheat in soils. Environmental Research, 2020, 188, 109736.	7.5	3
49	Do toxicokinetic and toxicodynamic processes hold the same for light and heavy rare earth elements in terrestrial organism Enchytraeus crypticus?. Environmental Pollution, 2020, 262, 114234.	7.5	16
50	The shuttling effects and associated mechanisms of different types of iron oxide nanoparticles for Cu(II) reduction by Geobacter sulfurreducens. Journal of Hazardous Materials, 2020, 393, 122390.	12.4	13
51	Elucidating Toxicodynamic Differences at the Molecular Scale between ZnO Nanoparticles and ZnCl ₂ in <i>Enchytraeus crypticus</i> via Nontargeted Metabolomics. Environmental Science & Technology, 2020, 54, 3487-3498.	10.0	43
52	Effective Modeling Framework for Quantifying the Potential Impacts of Coexisting Anions on the Toxicity of Arsenate, Selenite, and Vanadate. Environmental Science & amp; Technology, 2020, 54, 2379-2388.	10.0	14
53	Different alkaline minerals interacted with biomass carbon during pyrolysis: Which one improved biochar carbon sequestration?. Journal of Cleaner Production, 2020, 255, 120162.	9.3	60
54	Uptake of vegetable and soft drink affected transformation and bioaccessibility of lead in gastrointestinal track exposed to lead-contaminated soil particles. Ecotoxicology and Environmental Safety, 2020, 194, 110411.	6.0	11

Hao Qiu

#	ARTICLE Coherent toxicity prediction framework for deciphering the joint effects of rare earth metals (La and) Tj ETQq1 1	IF 0 784314	
55		8.2	
56	Roles of the mineral constituents in sludge-derived biochar in persulfate activation for phenol degradation. Journal of Hazardous Materials, 2020, 398, 122861.	12.4	65
57	Cadmium stable isotope variation in a mountain area impacted by acid mine drainage. Science of the Total Environment, 2019, 646, 696-703.	8.0	56
58	Phytotoxicity and oxidative effects of typical quaternary ammonium compounds on wheat (Triticum) Tj ETQq0 0	0 rgBT /Ov	verlock 10 Tf
59	Infiltration behavior of heavy metals in runoff through soil amended with biochar as bulking agent. Environmental Pollution, 2019, 254, 113114.	7.5	21
60	Physicochemical property and colloidal stability of micron- and nano-particle biochar derived from a variety of feedstock sources. Science of the Total Environment, 2019, 661, 685-695.	8.0	126
61	Pyrolysis-temperature depended quinone and carbonyl groups as the electron accepting sites in barley grass derived biochar. Chemosphere, 2019, 232, 273-280.	8.2	82
62	Different mechanisms between biochar and activated carbon for the persulfate catalytic degradation of sulfamethoxazole: Roles of radicals in solution or solid phase. Chemical Engineering Journal, 2019, 375, 121908.	12.7	113
63	The cation competition and electrostatic theory are equally valid in quantifying the toxicity of trivalent rare earth ions (Y3+ and Ce3+) to Triticum aestivum. Environmental Pollution, 2019, 250, 456-463.	7.5	19
64	Simultaneous attenuation of phytoaccumulation of Cd and As in soil treated with inorganic and organic amendments. Environmental Pollution, 2019, 250, 464-474.	7.5	36
65	Two years of aging influences the distribution and lability of metal(loid)s in a contaminated soil amended with different biochars. Science of the Total Environment, 2019, 673, 245-253.	8.0	57
66	Different dynamic accumulation and toxicity of ZnO nanoparticles and ionic Zn in the soil sentinel organism Enchytraeus crypticus. Environmental Pollution, 2019, 245, 510-518.	7.5	24
67	Phytotoxicity of individual and binary mixtures of rare earth elements (Y, La, and Ce) in relation to bioavailability. Environmental Pollution, 2019, 246, 114-121.	7.5	38

68	Occurrence and fate of colloids and colloid-associated metals in a mining-impacted agricultural soil upon prolonged flooding. Journal of Hazardous Materials, 2018, 348, 56-66.	12.4	58
69	Additive toxicity of zinc and arsenate on barley (<i>Hordeum vulgare</i>) root elongation. Environmental Toxicology and Chemistry, 2017, 36, 1556-1562.	4.3	6
70	Timeâ€dependent uptake and toxicity of nickel to <i>Enchytraeus crypticus</i> in the presence of humic acid and fulvic acid. Environmental Toxicology and Chemistry, 2017, 36, 3019-3027.	4.3	10
71	Development of electrostatic-based bioavailability models for interpreting and predicting differential phytotoxicity and uptake of metal mixtures across different soils. Environmental Pollution, 2017, 226, 308-316.	7.5	12
72	Nanospecific Phytotoxicity of CuO Nanoparticles in Soils Disappeared When Bioavailability Factors Were Considered. Environmental Science & Technology, 2017, 51, 11976-11985.	10.0	51

ΗΑΟ QIU

#	Article	IF	CITATIONS
73	Effects of an iron-silicon material, a synthetic zeolite and an alkaline clay on vegetable uptake of As and Cd from a polluted agricultural soil and proposed remediation mechanisms. Environmental Geochemistry and Health, 2017, 39, 353-367.	3.4	44
74	Effect of coexisting Al(III) ions on Pb(II) sorption on biochars: Role of pH buffer and competition. Chemosphere, 2016, 161, 438-445.	8.2	28
75	Interactions and Toxicity of Cu–Zn mixtures to <i>Hordeum vulgare</i> in Different Soils Can Be Rationalized with Bioavailability-Based Prediction Models. Environmental Science & Technology, 2016, 50, 1014-1022.	10.0	40
76	A generic biotic ligand model quantifying the development in time of Ni toxicity to Enchytraeus crypticus. Chemosphere, 2015, 124, 170-176.	8.2	7
77	Statistically significant deviations from additivity: What do they mean in assessing toxicity of mixtures?. Ecotoxicology and Environmental Safety, 2015, 122, 37-44.	6.0	16
78	Incorporating bioavailability into toxicity assessment of Cu-Ni, Cu-Cd, and Ni-Cd mixtures with the extended biotic ligand model and the WHAM-F tox approach. Environmental Science and Pollution Research, 2015, 22, 19213-19223.	5.3	20
79	Can commonly measurable traits explain differences in metal accumulation and toxicity in earthworm species?. Ecotoxicology, 2014, 23, 21-32.	2.4	21
80	Modeling cadmium and nickel toxicity to earthworms with the free ion approach. Environmental Toxicology and Chemistry, 2014, 33, 438-446.	4.3	4
81	A Fuzzy-based Methodology for an Aggregative Environmental Risk Assessment of Restored Soil. Pedosphere, 2014, 24, 220-231.	4.0	8
82	Modelling uptake and toxicity of nickel in solution to Enchytraeus crypticus with biotic ligand model theory. Environmental Pollution, 2014, 188, 17-26.	7.5	15
83	Predicting Copper Toxicity to Different Earthworm Species Using a Multicomponent Freundlich Model. Environmental Science & Technology, 2013, 47, 4796-4803.	10.0	34
84	Attenuation of Metal Bioavailability in Acidic Multi-Metal Contaminated Soil Treated with Fly Ash and Steel Slag. Pedosphere, 2012, 22, 544-553.	4.0	38
85	Mitigation effects of silicon rich amendments on heavy metal accumulation in rice (Oryza sativa L.) planted on multi-metal contaminated acidic soil. Chemosphere, 2011, 83, 1234-1240.	8.2	256
86	Interactions of cadmium and zinc impact their toxicity to the earthworm <i>Aporrectodea caliginosa</i> . Environmental Toxicology and Chemistry, 2011, 30, 2084-2093.	4.3	33
87	Cadmium tolerance of carbon assimilation enzymes and chloroplast in Zn/Cd hyperaccumulator Picris divaricata. Journal of Plant Physiology, 2010, 167, 81-87.	3.5	132
88	Acid deposition critical loads modeling for the simulation of sulfur exceedance and reduction in Guangdong, China. Journal of Environmental Sciences, 2009, 21, 1108-1117.	6.1	2